CHAPTER - 3

REFRACTIVE INDEX, BAND GAP ENERGY, DIELECTRIC CONSTANT AND POLARIZABILITY CALCULATIONS OF FERROELECTRIC ETHYLENEDIAMINIUM TETRACHLOROZINCATE CRYSTAL

3.1 Introduction

In earlier decades, crystals of the type A_2B_4 (where A = monovalent cation, NH_4^+ and its alkyl derivatives; B = bivalent transition metal cation) revealed an interesting field for studies owing to the occurrence of paraelectric-incommensurate-commensurate-ferroelectric phase transitions [**87-92**]. Later, a slight modification on these type of materials was carried out by adding the halogen group atoms such as A_2BX_4 (where X = halogen) that attracted a lot of attention due to the possibility of many successive phase transitions including incommensurate-commensurate phase ones together with their unusual physical properties [**93-95**]. These compounds represent the largest known group of insulating crystals with structurally incommensurate phases [**96, 97**]. Among these materials, zincates family materials especially Tetramethylammonium Tetracholorozincate ($[N(CH_3)_4]_2ZnCl_4$) and BisTetraethylammoniun Tetracholorozincate ($[N(C_2H_5)_4]_2ZnCl_4$) have been widely studied for their structural phase transitions by various researchers using a variety of techniques in the past three decades [**98-104**]. Some focus on the spectroscopic features and thermal investigations of this type of materials is also found [**95, 105, 106**] in this series. Very few works concentrate on the polarizability and optical band gap energy of the zincates family materials of the type A_2BX_4 [**107]**. Apart from this type of materials similar studies on the optical properties of sodium acid phthalate

ferroelectric material had been carried out **[108]**. The optical properties of these organic inorganic hybrid metal halide (A_2BX_4) ferroelectric materials find wide range of applications in laser devices. However, an extensive analysis of the optical constants such as band gap energy, extinction coefficient, refractive index and dielectric permittivity along with the polarizbility of these ferroelectric materials is hardly found till date.

In the present work, we analyse and report the optical constants of Ethylenediaminium Tetrachlorozincate ($(C_2H_{10}N_2)^{2+}[ZnCl_4]^{2-}$) crystal which is one of the members of zincates (A_2ZnCl_4) family. Furthermore, vibrational spectroscopic characterization and dielectric properties of the material are also addressed. From the obtained dielectric constant values, the polarizability of the material is calculated using Clausius–Mossotti equation. Theoretically, Penn analysis has also been made to support the obtained polarizability value in Clausius–Mossotti equation. In addition, Plasmon energy and Fermi energy are also determined through Penn analysis.

3.2 Materials and methods

All the materials used in the present study were of pure grade procured from Sigma Aldrich. The crystals under study were crystallized by slow evaporation method as given in the literature **[109]**. Crystals suitable for single crystal X – ray diffraction were selected and the lattice parameters were determined using Enraf – Nonius CAD – 4 diffractometer with CuK_α radiation. FT – IR spectrum of the crystals were recorded in the wavenumber ranging from 4000 – 400 cm^{-1} (Thermo Nicolet, Avatar 370). Raman spectra of powder samples were measured using a micro Raman spectrometer (Renishaw, UK, model inVia) with 514 nm laser

excitation from 1 cm^{-1} to 4000 cm^{-1}. The UV – Vis reflectance and transmittance spectra were recorded using Cary– 300 instrument in the range 200-1100 nm (in terms of frequencies in the range of 1.4×10^{15}-2.7×10^{14} Hz) with the resolution 1 nm. The dielectric measurements were carried out using N4L Numetric Q PSM 1735 instrument in the frequency range 1kHz-10MHz at room temperature. A polished grown crystal coated with silver paste was used to measure the capacitance. The crystal area which was used for this measurement was 0.21 mm^2 (0.7 mm×0.3 mm). The Radiant Technology method (Tester Name: PMF0713-334) was used for hysteresis loop study. The pelletized crystal of thickness 1.25 mm and area 1.32 cm^2 was used for this measurement at room temperature.

3.3 Results and Discussion

3.3.1 Confirmation of the material

3.3.1.1 Single crystal XRD study

The grown crystal ($(C_2H_{10}N_2)^{2+}[ZnCl_4]^{2-}$) is subjected to single crystal XRD study to obtain the lattice parameters and volume of the unit cell. The obtained parameters are a = 6.206 (3)Å, b = 12.882(1)Å and c= 19.108(2)Å and V= 1527(2)$Å^3$ which agree reasonably with the literature values **[110]** and reveal the orthorhombic structure with the symmetry P_{212121} (D_2^4) of the material.

3.3.1.2 Vibrational studies

The recorded FTIR and Raman spectra are displayed in **Figs. 3.1 and 3.2** respectively and the vibrational assignments are listed in **Table 3.1**. The asymmetric CH_3 stretching vibration peak is found to have a weak intensity as observed at 3028 cm^{-1} in FTIR and a medium peak in Raman at 3038 $cm^{-1.}$ The peaks that appeared at 2577 and 2499 cm^{-1} in IR spectrum are assigned to C-H stretching of CH_3.

Table 3.1 Selected vibrational assignments

Wavenumber		Assignments
FT-IR (cm^{-1})	Raman (cm^{-1})	
3028	3038	Asym. stret. of CH_3
2577	-	C-H sym. stret. of CH_3
2499	-	C-H sym. stret. of CH_3
2197	2228	C-H and N-H asym. stret.
1927	-	C-H and N-H sym. stret.
1485	1497	Def. of CH_2
1440	1442	Def. of CH_2
1375	-	Wagg. of CH_2
1321	1338	Wagg. of CH_2
1213	-	Twist. of CH_2

Wavenumber		Assignments
FT-IR (cm^{-1})	Raman (cm^{-1})	
1171	-	Rock. of CH_2
1124	1123	Rock. of CH_2
1030	1036	C-C stret.
963	964	
894	901	Rock. of CH_3
809	813	
623	-	Ethylene twisting
543	-	Ethylene twisting
469	-	Skeletal vibration
	281	
	218	
	146	Internal vibrations of $ZnCl_4^{2-}$
	106	
	83	

The peaks found at 963 and 894 cm^{-1} in FTIR and at 964 and 901 cm^{-1} in Raman are assigned to CH_3 rocking vibrations. The assignments for N-H and C-H asymmetric stretching vibrations are given to the peaks observed at 2197 cm^{-1} in FTIR and at 2228 cm^{-1} in Raman, while the peak at 1927 cm^{-1} in IR is assigned to N-H and C-H symmetric stretching vibrations. Considering the CH_2 group vibrations, the deformation of CH_2 is observed at 1485 and 1440 cm^{-1} in FTIR and at 1497 and 1442 cm^{-1} in Raman. The peaks at 1375 and 1321 cm^{-1} in IR are assigned to CH_2 wagging vibration and it is at 1338 cm^{-1} in Raman. The CH_2 twisting vibration mode is found at 1213 cm^{-1} in FTIR. The observed peaks at 1171, 1124 and 809 cm^{-1} in FTIR correspond to CH_2 rocking vibrations and in Raman it is at 1123 and 813cm^{-1}. C-C stretching is identified at 1030 cm^{-1} in IR and at 1036 cm^{-1} in Raman. Further, the peak that appeared at 469 cm^{-1} is assigned to skeletal vibration and the peaks at 623 and 543 cm^{-1} are assigned to ethylene twisting vibrations. The low frequency Raman absorption peaks occurring at 281, 218, 146, 106 and 83 cm^{-1} are due to internal vibrations of $ZnCl_4^{2-}$ ion **[106, 110]**.

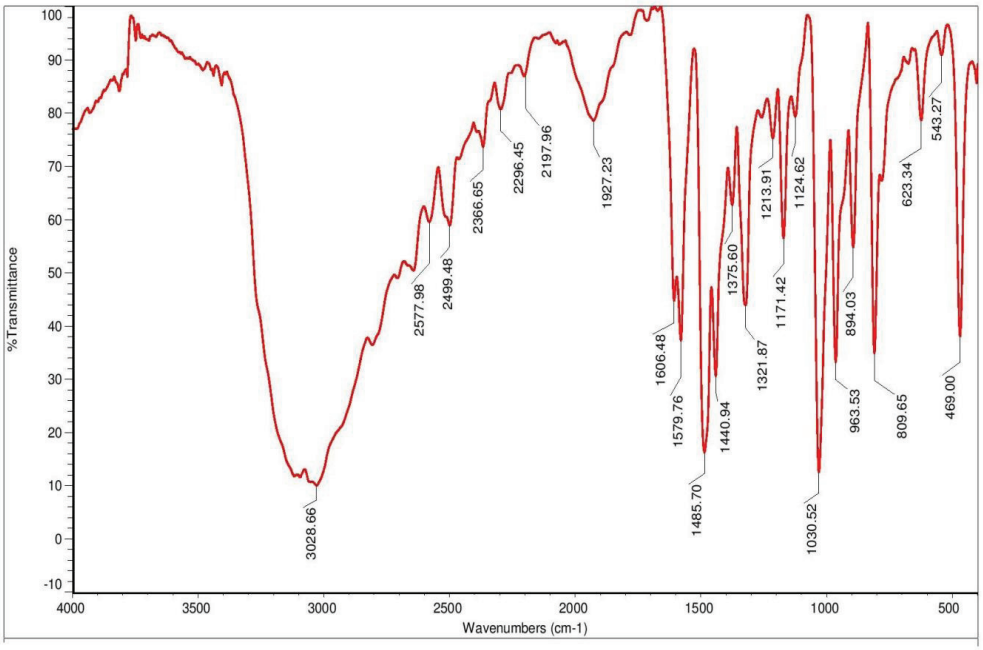

Fig. 3.1 FTIR spectrum

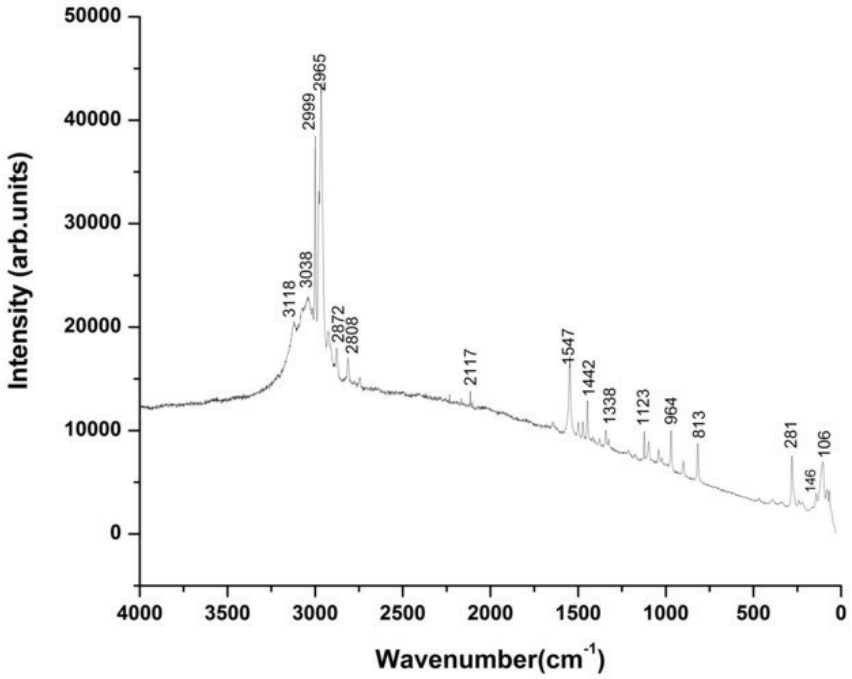

Fig. 3.2 Raman spectrum

3.3.2 Optical studies

The spectral distribution of Transmission T (λ) in the wavelength range 200 – 1100 nm is displayed in **Fig. 3.3**. It could be noted that the transmittance is not uniform in the whole wavelength range. High transmittance is observed in the visible region (400-700 nm). From the recorded transmittance values the absorption coefficient (α) is calculated using the following relation

$$\alpha = \frac{ln^{1}/_{T}}{t} \tag{1}$$

where, t is the thickness of the crystal.

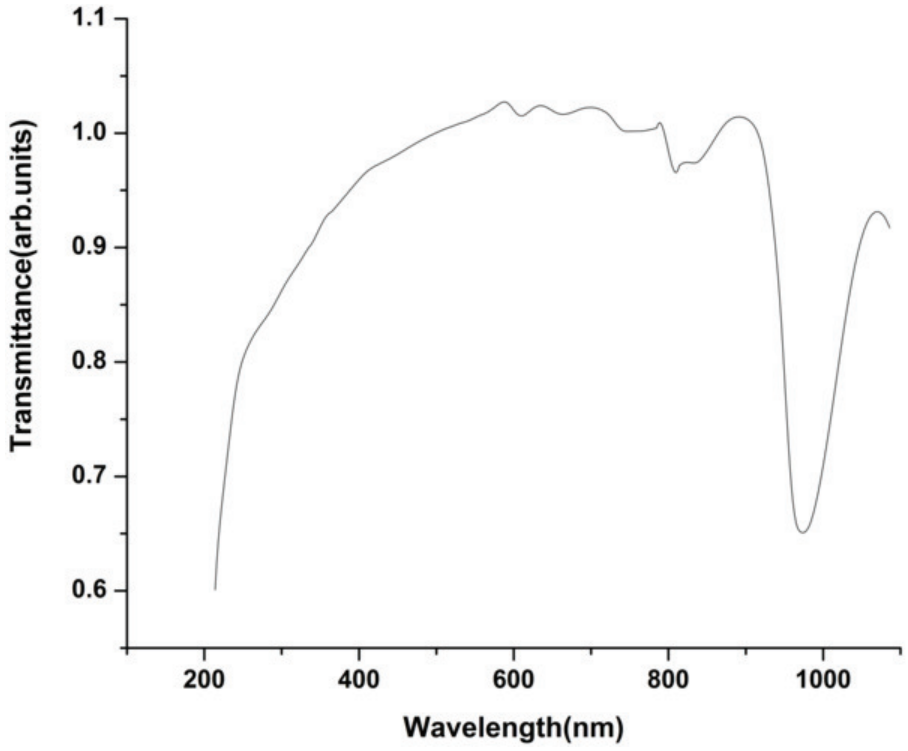

Fig. 3.3 Recorded Transmittance spectrum

The variation of absorption coefficient as a function of incident wavelength is portrayed in **Fig. 3.4**. It has been observed that the absorption coefficient values

monotonically decrease with the increase of wavelength. There is no absorption found in the visible region and it predicts the insulating behaviour of the material. The maximum absorption peak found at the IR region (974 nm) could be attributed to the atomic vibrations of the crystals and therefore it cannot correspond to any transitions. Since this absorption is analogue to the infrared absorption due to vibrations in polar molecules it is called as phonon absorption **[111]**. The absorption coefficient values are in the order of 10^2 m^{-1} and it indicates the indirect allowed transition of the material **[112]**. The optical band gap energy is determined from the absorption coefficient values using Tauc relation **[113]**

$$\alpha h\nu = A\left(h\nu - E_g\right)^n \tag{2}$$

where, $h\upsilon$ is the photon energy, α is the absorption coefficient, E_g is the band gap and A is a constant. The value of n = ½ for direct allowed transition and 2 for indirect allowed transition. For indirect allowed transition the eqn.(2) is slightly modified as **[114]**

$$\alpha h\nu = A\left(h\nu - E_g \pm E_p\right)^n \tag{3}$$

where E_p is the lattice phonon energy.

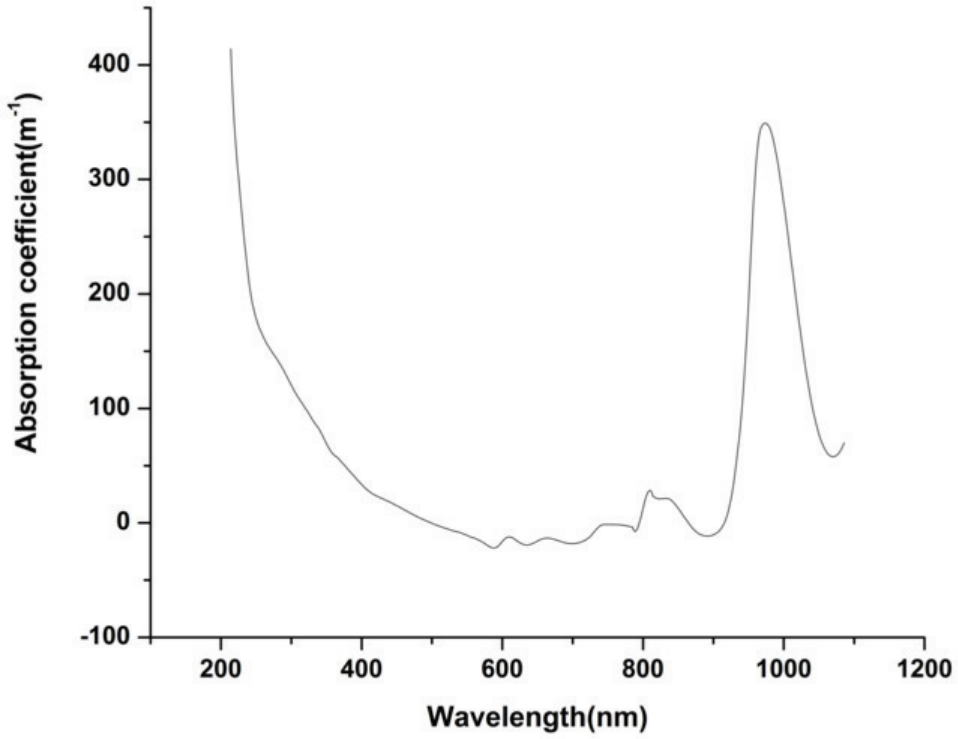

Fig. 3.4 Calculated Absorption coefficient plot

In our case, the material exhibits an indirect allowed transition and hence *n* is equal to 2. Intercept on $x - axis$ corresponds to zero absorption coefficient in Tauc plot ($hv\ vs(\alpha hv)^{1/2}$) which gives the optical band gap energy value. The observed bandgap energy value of Ethyelenediaminium Tetracholorozincate is 3.92 eV (**Fig. 3.5**) and it suggests the insulating behaviour of the material. Hence, it is likely that this material responds to dielectric behaviour. In addition, there is only one straight line that is observed in the Tauc plot which indicates the lattice phonon energy $E_p \approx 0$ for our material.

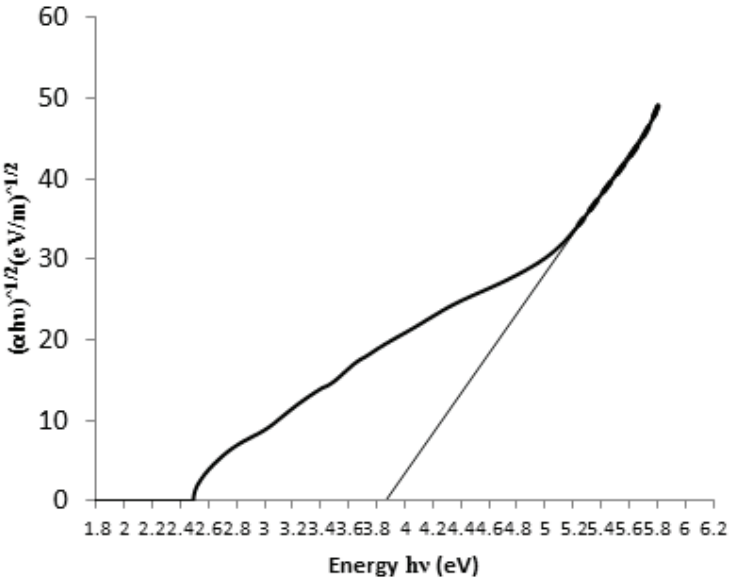

Fig. 3.5 Tauc plot (Band gap energy determination)

Since the absorption coefficient values are nearly zero in the range 300-900 nm, the extinction coefficient (k) which correlates to the absorption coefficient as $k = \alpha\lambda/4\pi$ should be zero for insulating materials. **Fig. 3.6** could be the evidence for this prediction. The values of refractive index (n) have been calculated using the theory of reflectivity of light. According to this theory, the reflectance (R) can be expressed by Fresnel's coefficients **[115, 116]**

$$R = \frac{(n-1)^2+k^2}{(n+1)^2+k^2} \tag{4}$$

For insulating materials this equation is simplified as

$$R = \frac{(n-1)^2}{(n+1)^2} \tag{5}$$

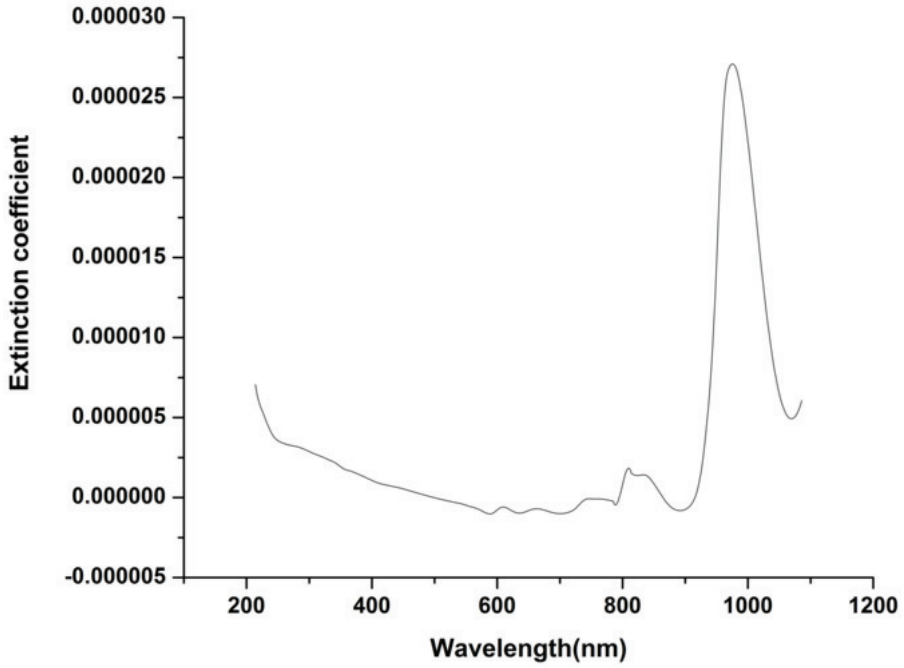

Fig. 3.6 Calculated extinction coefficient plot

The calculated value of refractive index with the variation of wavelength is displayed in **Fig. 3.7**. The Refractive index monotonically increases with the increase of wavelength. It is interesting to observe the values of refractive index as these lie in the range of refractive indices of the known ferroelectric materials **[117-121]**. The value of refractive index at 470 nm is 3.4 whereas it is 3.10 at the same wavelength for the ferroelectric material $PbTiO_3$ **[122]** at room temperature. Hence it predicts the possibility of ferroelectric behaviour of the studied material.

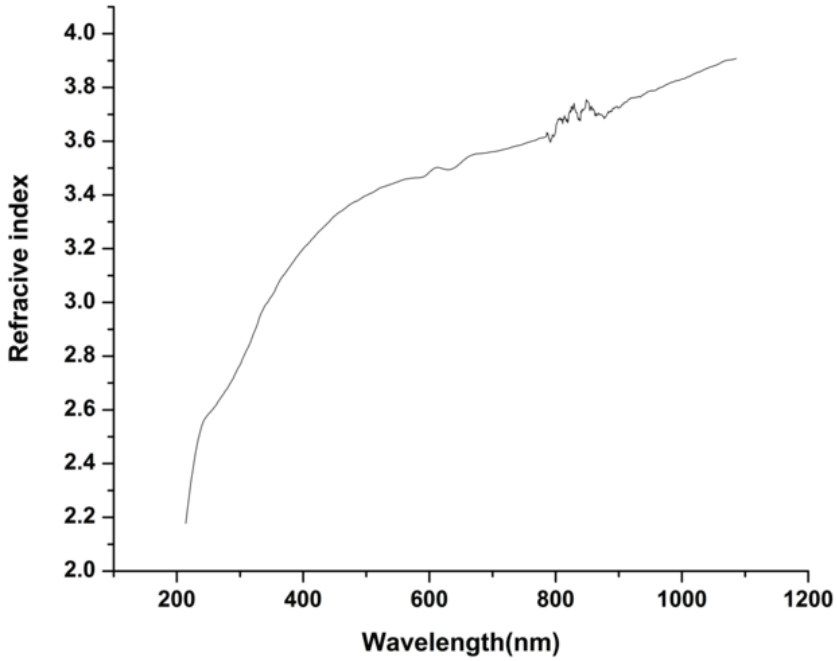

Fig. 3.7 Calculated Refractive index plot

Further, the real and imaginary dielectric functions ($\boldsymbol{\varepsilon'}, \boldsymbol{\varepsilon''}$) also play a vital role in the optical properties. They have been calculated as follows

$$\varepsilon' = n^2 - k^2 \tag{6}$$

$$\varepsilon'' = 2nk \tag{7}$$

Since k =0, the imaginary dielectric function tends to zero whereas the real dielectric function can be$\boldsymbol{\varepsilon' = n^2}$**.** When compared with refractive index values (**Fig. 3.7**), it is noticeable that the real dielectric constant value (**Fig. 3.8**) is the square of the refractive index to satisfy the relation $\boldsymbol{\varepsilon' = n^2}$. It is observed that the values of dielectric constant lie in the range 4-16 and there is a steady decrease in dielectric constant values with the increasing values of frequencies.

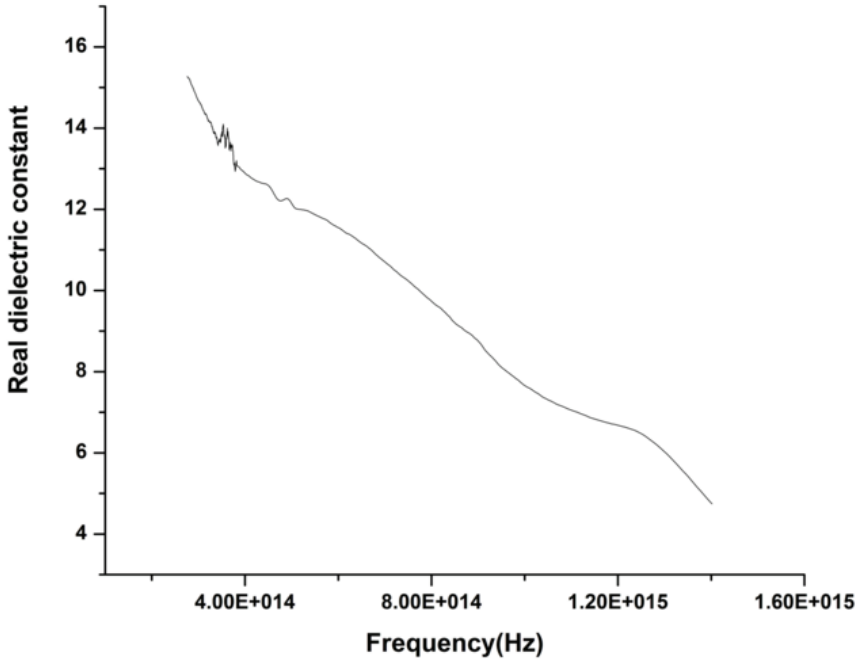

Fig. 3.8 Variation of calculated Real Dielectric constants with optical frequencies

The polarizability due to the contribution of applied external electric field (electronic polarizability) in the optical region (high frequency region) is calculated using the calculated real dielectric constant values by Clausius-Mosotti equation **[123]** as follows

$$\alpha \simeq \left[\frac{\varepsilon_r - 1}{\varepsilon_r + 2}\right]\left[\frac{M}{\rho}\right] / 2.53 \times 10^{24} cm^3 \quad (8)$$

where M is the molecular weight (269.29) and ρ is the density (1.862 Mg m^{-3})of the crystal. The calculated polarizabilities are in the range 3×10^{-23}- 4.8×10^{-23} cm^3. The increase of polarizability with increasing frequencies is observed in **Fig. 3.9**.

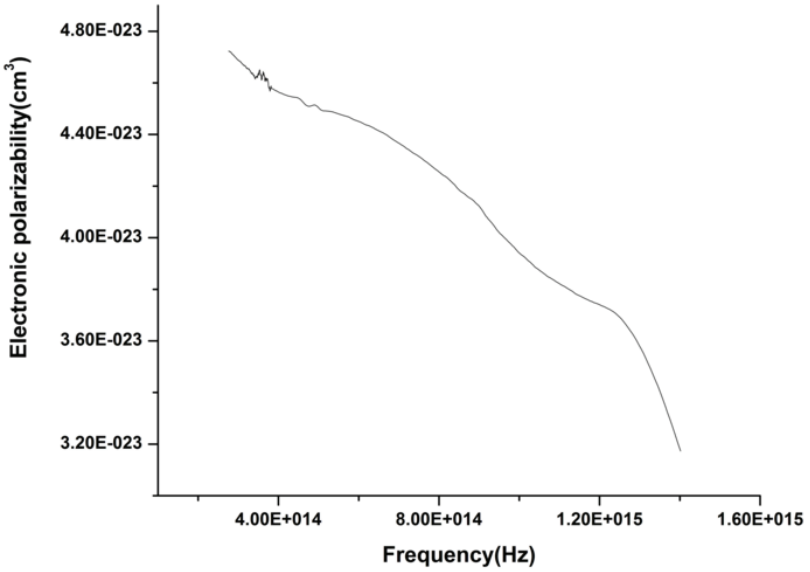

Fig. 3.9 Electronic polarizability in optical region

3.3.3 Dielectric studies

Dielectric properties of the materials are based on the interaction of an external field with the electric dipole moment of the sample. The frequency dependent dielectric loss of the material is portrayed in **Fig. 3.10**. The lesser value of dielectric loss implies the reasonably good quality of the crystal. Since the crystal area is lesser than the electrode area, from the measured capacitance values of the crystal and air, the dielectric constant values of the crystals are calculated by using the following equation

$$\varepsilon_r = \frac{\left[C_{cry} - C_{air}\left(\frac{1-A_{cry}}{A_{air}}\right)\right]}{C_{air}} \frac{A_{air}}{A_{cry}} \tag{9}$$

where C_{crys} is the capacitance of the crystal. C_{air} is the capacitance of the air of the same dimension as the crystal, A_{crys} and A_{air} represent the area of the crystal and area of the electrode respectively **[124]**.

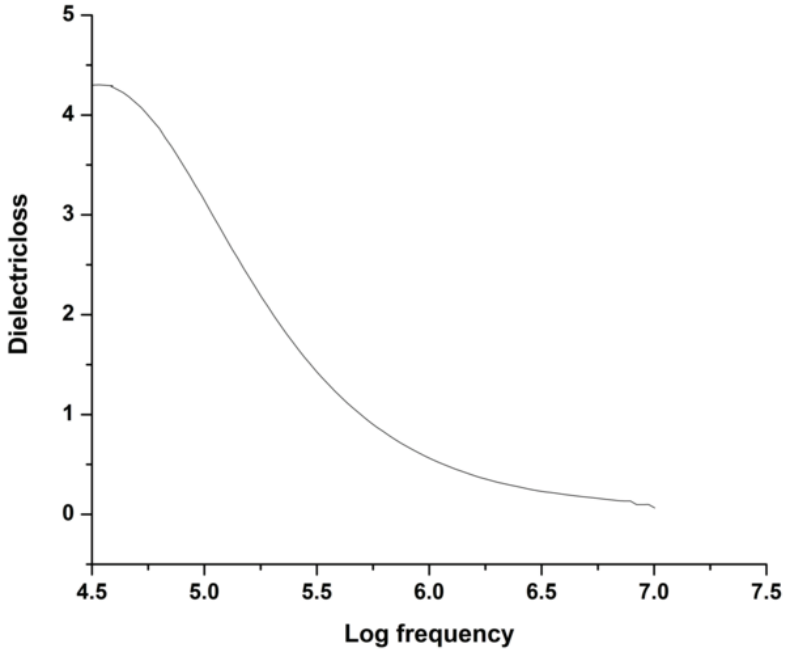

Fig. 3.10 Variation of dielectric loss with respect to frequency

The variation of dielectric constant against frequency in the audio frequency region (1000-10000 Hz) is shown in **Fig. 3.11**. The dielectric constant values drastically decrease with the increasing of frequency in this region. The dielectric constant is very high at lower frequency regions contrary to the optical frequency region (high frequency) because of the contribution of all polarizability components namely dipolar, space charge, ionic and electronic. The higher value of dielectric constant (in the order of 10^3) than the usual dielectric material confirms that the studied material is ferroelectric in nature **[125]**.

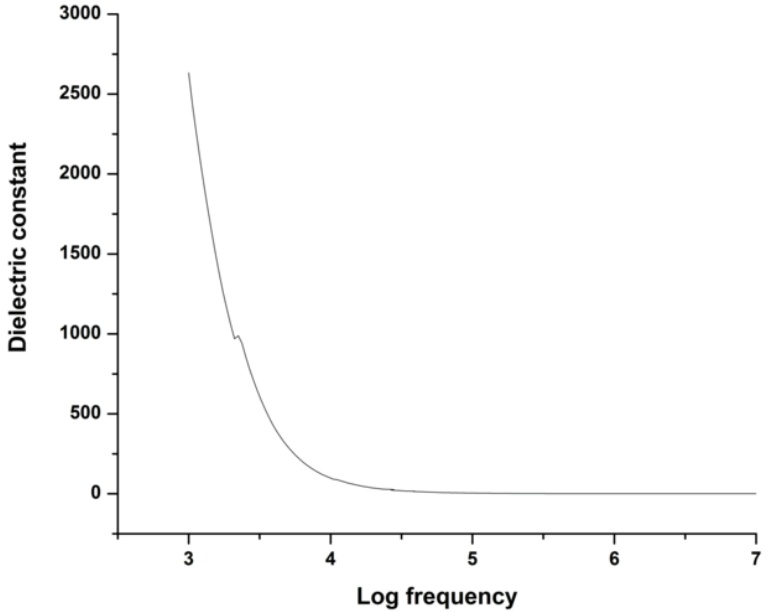

Fig. 3.11 Dielectric constant variations in the lower frequencies

From the calculated dielectric constant values, the polarizability of the material due to the contribution of all polarizability components is calculated by Clausius-Mosotti equation. The average polarizability is found to be 5.706×10^{-23} cm^3. On comparison with electronic polarizability values, it is concluded that electric field contributes a major part in the determination of total polarizability value.

3.3.4 Ferroelectric hysteresis loop study

The electric field response of polarization is displayed in **Fig. 3.12** for fixed voltages of 10, 50 and 90V. The hysteresis loop obtained shows the ferroelectric nature of the material. It is observed that the remanant polarization (P_r) gets increased with the increase of applied voltage. Moreover, there is a resistive leakage along grain boundaries which is identified in the hysteresis loop at the mentioned voltages. It suggests the material is ferroelectric ceramic like the already known

inorganic Perovskite structure materials $BaTiO_3$ and $PbTiO_3$. Further it indicates the best suitability of the material as a capacitor since it is ferroelectric ceramic.

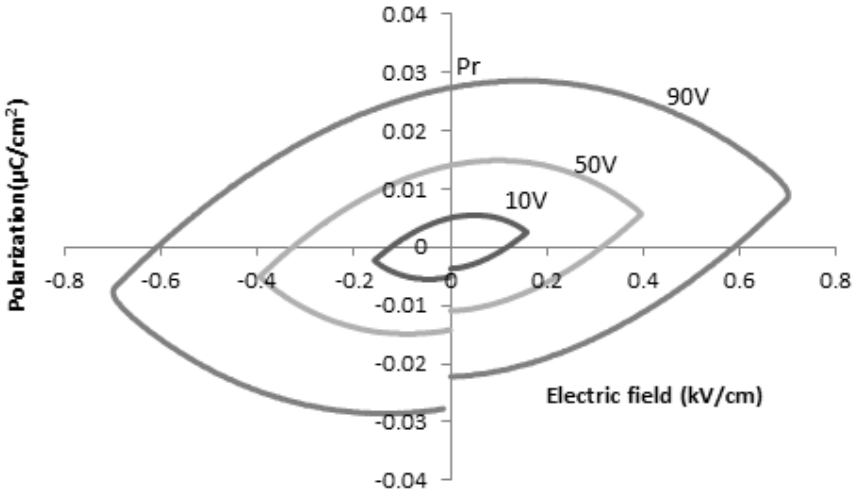

Fig. 3.12 Ferroelectric Hysteresis loop

3.3.5 Penn analysis

Penn analysis **[126, 127]** focuses on the dielectric constant and its related properties of the wide band gap semiconductors. In general, the dielectric constant explicitly depends on the plasmon energy, average gap (Penn gap) and the Fermi energy. The Penn gap is determined by fitting the dielectric constant (ε_∞)with the plasmon energy. An attempt is made on the use of Penn analysis for our insulating material to find the total polarizability value with the obtained high value of dielectric constant from the dielectric studies.

The valence electron Plasmon energy ($\hbar\omega$) is given by

$$\hbar\omega = 28.8\sqrt{\frac{Z\rho}{M}}\ (eV) \qquad (10)$$

where, Z is the total number of valence states(Z = 38 for our material), ρ is the density and M is the molecular weight of the crystal.

The Fermi energy E_F is calculated as follows using $\hbar\omega$

$$E_F = 0.2947(\hbar\omega)^{\frac{4}{3}}(eV) \quad (11)$$

The polarizability α is obtained as

$$\alpha = \left[\frac{(\hbar\omega)^2 S_0}{(\hbar\omega)^2 S_0 + 3E_p^2}\right]\frac{M}{\rho}0.396 \times 10^{-24} cm^3 \quad (12)$$

where E_p is the Penn gap and S_0 is a constant for the material which are defined by

$$E_p = \frac{\hbar\omega}{(\varepsilon_r - 1)^{1/2}}\ (eV) \quad (13)$$

$$S_0 = 1 - \frac{E_p}{4E_F} + \frac{1}{3}\left(\frac{E_p}{4E_F}\right)^2 \quad (14)$$

The calculated Plasmon energy is 14.76 eV and Fermi energy is 10.676 eV. Since the constant $S_0 = 1$ for the original Penn model, we have to concentrate only on the polarizability values that correspond to S_0 whose value is nearly equal to "1". For our material the average S_0 is 0.991 and the average polarizability is found to be 5.717×10^{-23} cm^3 which agrees well with the polarizability value obtained from Clausis-Mossotti equation.

3.4 Summary and Conclusion

The ferroelectric Ethylenediaminium Tetrachlorozincate ($(C_2H_{10}N_2)^{2+}[ZnCl_4]^{2-}$) crystal is synthesized by slow evaporation method. The functional groups such as CH_3, CH_2 and N-H vibrations in the material are identified both in FTIR and Raman studies and $ZnCl_4$ vibrations are identified in Raman. Together with the vibrational analysis, single crystal XRD study confirms the formation of the material in orthorhombic structure. The absence of absorption in the

visible region is identified from UV-Vis studies and the absorption coefficient values (in the order of 10^2 m^{-1}) suggest the indirect bang gap nature of the material. The optical bandgap energy is found to be 3.92 eV from Tauc plot and it implies the insulating behaviour of the material. The zero value of extinction coefficient supports the insulating behaviour and it leads to the absence of imaginary dielectric function. The calculated refractive index at 470 nm is 3.4 and agrees with the refractive index of the ferroelectric material $PbTiO_3$ at the same wavelength. The real dielectric constant is derived from the refractive index values. The electronic polarizability is calculated from the real part of the dielectric constant values using the Clausius-Mossotti equation in the optical frequency region and it is found to be in the range 3×10^{-23}- 4.8×10^{-23} cm^3.The ferroelectric behaviour is confirmed by the large value of dielectric constant (nearly in the order of 10^3) obtained through dielectric studies. The obtained hysteresis loop from Radiant Technology method strongly supports the ferroelectric ceramic behaviour of the material. The experimentally calculated polarizability value (5.706×10^{-23} cm^3) due to the contribution of all polarizability components(space charge, dipolar, ionic and electronic) is matches well with the theoretically calculated value (5.717×10^{-23} cm^3) through Penn analysis. The electronic polarizability contribution is identified as a major part in the determination of total polarizability.